의학박사 학위논문

Human chorionic plate-derived mesenchymal stem cells restore hepatic lipid metabolism in a rat model of bile duct ligation

담관결찰 쥐에서 태반유래줄기세포 이식의 간 지질대사 개선 효과

2018년 2월

서울대학교 대학원
의학과 줄기세포생물학 전공
이 윤 빈

A thesis of the Degree of Doctor of Philosophy

Human chorionic plate-derived mesenchymal stem cells restore hepatic lipid metabolism in a rat model of bile duct ligation

February 2018

Seoul National University
Stem Cell Biology
Yun Bin Lee

담관결찰 쥐에서 태반유래줄기세포 이식의 간 지질대사 개선 효과

지도교수 **윤 정 환**

이 논문을 의학박사 학위논문으로 제출함

2017년 10월

서울대학교 대학원

의학과 줄기세포생물학 전공

이 윤 빈

이윤빈의 의학박사 학위논문을 인준함

2017년 12월

위 원 장	(인)
부위원장	(인)
위 원	(인)
위 원	(인)
위 원	(인)

Human chorionic plate-derived mesenchymal stem cells restore hepatic lipid metabolism in a rat model of bile duct ligation

by

Yun Bin Lee, M.D.

A Thesis Submitted to the Department of Stem Cell Biology
in Partial Fulfillment of the Requirements
for the Degree of Doctor of Philosophy in Medicine
at the Seoul National University College of Medicine

December, 2017

Approved by thesis committee:

Professor	_____	Chairman
Professor	_____	Vice Chairman
Professor	_____	
Professor	_____	
Professor	_____	

Abstract

Human chorionic plate-derived mesenchymal stem cells restore hepatic lipid metabolism in a rat model of bile duct ligation

Yun Bin Lee

Department of Stem Cell Biology

Seoul National University College of Medicine

In cholestatic liver diseases, impaired bile excretion disrupts lipid homeostasis. We investigated changes of lipid metabolism, including mitochondrial β-oxidation, in a rat model of bile duct ligation (BDL) in which chorionic plate-derived mesenchymal stem cells (CP-MSCs) were transplanted. The concentration of serum cholesterol, which was elevated after BDL, was significantly decreased following transplantation of CP-MSCs. The expression levels of genes involved in intracellular lipid uptake, including long-chain fatty acyl-CoA synthetases and fatty acid transport proteins, were decreased in rats after BDL, however, were not significantly changed by subsequent CP-MSC transplantation. Carnitine palmitoyltransferase 1A (CPT1A), a rate-limiting enzyme in mitochondrial β-oxidation, was upregulated after BDL and then was downregulated after CP-MSC transplantation. CPT1A expression was changed via microRNA-33–a posttranscriptional regulator of CPT1A–in a peroxisome proliferator-activated receptor α-independent manner. Cellular adenosine triphosphate production–an

indicator of mitochondrial function–was reduced after BDL and was restored by CP-MSC transplantation. Expression levels of heme oxygenases also were significantly affected following BDL and CP-MSC transplantation. Lipid metabolism is altered in response to chronic cholestatic liver injury and can be restored by CP-MSC transplantation. Our study findings support the therapeutic potential of CP-MSCs in cholestatic liver diseases and help understanding fundamental mechanism by which CP-MSCs affect energy metabolism.

Key words: Cholestasis, bile duct ligation, CP-MSCs, lipid metabolism, fatty acid oxidation, CPT1A, microRNA-33

Student Number: 2015-30001

List of Tables

List of Figures

Contents

Introduction

Cholestatic liver injury, which is caused by accumulation of bile acids and lipids, comprises a wide spectrum ranging from acute transient hepatitis to cirrhosis with portal hypertension [1-3]. The liver controls central processes of lipid metabolism including fatty acid synthesis, mitochondrial β-oxidation, and phospholipid transport. Impaired bile excretion, caused by biliary obstruction or liver damage, disrupts cholesterol and phospholipid metabolism [4]. In a rat model of bile duct ligation (BDL), serum levels of very low-density lipoprotein cholesterol, low-density lipoprotein (LDL) cholesterol are drastically elevated, whereas hepatic lipid concentrations are unchanged [5]. However, alterations in mitochondrial function in chronic cholestatic liver diseases have not been elucidated.

Mesenchymal stem cells (MSCs) are multipotent adult stem cells that can differentiate into various cell types of the three germ layers (i.e., the ectoderm, mesoderm, and endoderm) [6]. The human placenta is an abundant source of MSCs. Placenta-derived MSCs (PD-MSCs) which originate from the fetus possess great potential for self-renewal, proliferation, and differentiation [7, 8]. We previously found that full-term placenta harbors several types of PD-MSCs, including chorionic plate-derived MSCs (CP-MSCs), chorionic villi-derived MSCs, and Wharton's jelly-derived MSCs [9]. CP-MSCs are highly capable of differentiating into various lineage cells, including hepatocytes. Moreover, CP-MSCs have been demonstrated to have anti-inflammatory, anti-fibrotic, and proregenerative

properties in the damaged liver [10, 11].

We therefore used a BDL rat model of chronic cholestatic liver injury to clarify the alterations in hepatic lipid homeostasis–focusing on mitochondrial dysfunction–and the impact of CP-MSC transplantation restoring the alterations in hepatic lipid metabolism.

Materials and Methods

Cell Culture

Collection of placenta samples for research purposes was approved by the Institutional Review Board of CHA Gangnam Medical Center, Seoul, Korea (IRB 07-18). All participants provided written informed consent prior to sample collection. Placentas were obtained from women who were free of any medical, obstetrical, or surgical complications and who delivered at term (38±2 gestational weeks). CP-MSCs were isolated as described previously [10] and were cultured in Dulbecco's modified Eagle medium/Ham's F-12 medium (DMEM/F12; Sigma-Aldrich, St. Louis, MO, USA) supplemented with 10% fetal bovine serum (FBS; Sigma-Aldrich), 1% penicillin/streptomycin (Sigma-Aldrich), 1 μg/mL heparin (Sigma-Aldrich), and 25 ng/mL human fibroblast growth factor-4 (hFGF-4; Peprotech, Inc., Rocky Hill, NJ, USA) at 37°C in a 5% CO_2 incubator containing 20% O_2.

BDL Rat Model and Transplantation of CP-MSCs

Male 7-week-old Sprague-Dawley rats (Orient Bio Inc., Seongnam, Korea) were maintained in an air-conditioned animal facility. The common bile duct was ligated under general anesthesia with Avertin (2,2,2-tribromoethanol, Sigma-Aldrich) as described previously [12, 13]. One week after BDL, CP-MSCs (2×10^6 cells, 8–10 passages) were injected intravenously via tail vein in the transplanted group. CP-

MSC number was determined based on the previous dose determining experiments [10, 14]. Liver tissues and blood samples were collected 1, 2, 3, and 5 weeks post-transplantation in the transplanted group and 1, 2, 3, and 5 weeks post-BDL in the nontransplanted group. The experimental protocols were approved by the Institutional Animal Care and Use Committee of CHA University, Seongnam, Korea (IACUC-140009).

Histological Analysis

Liver tissue samples were fixed in 10% formalin, embedded in paraffin, and sectioned at 5 μm-thickness. Sections then were stained with hematoxylin and eosin and observed under light microscopy at 200× magnification (Axioskop2, Carl Zeiss Micro-Imaging, Oberkochen, Germany).

Immunofluorescence Staining

To analyze the expression of carnitine palmitoyltransferase 1A (CPT1A) in liver tissues, 6 μm-thick cryostat sections were incubated with a protein blocking solution (Dako, Glostrup, Denmark) for 40 minutes at room temperature. Then, mouse anti-CPT1A antibody (1:100, Abcam, Cambridge, MA, USA) was treated, and sections were incubated at 4°C overnight. After washing with phosphate-buffered saline (PBS), samples were incubated with Alexa 488-conjugated secondary antibody (1:150, Invitrogen, Carlsbad, CA, USA) for 1 hour at room temperature. Sections then were stained with 4’,6-diamidino-2-phenylindole

(DAPI) for nuclear counterstaining and were observed under fluorescence microscopy 400× magnification (Nikon, Tokyo, Minato, Japan).

Blood Chemistry

The serum concentrations of total cholesterol, high-density lipoprotein (HDL) cholesterol, LDL cholesterol, triglyceride, albumin, total bilirubin, alkaline phosphatase (ALP), aspartate transaminase, alanine transaminase, and C-reactive protein (CRP) were measured enzymatically by an automated analyzer (Hitachi 747, Hitachi, Tokyo, Japan).

Fatty Acyl-CoA Synthetase Activity Assay

Long-chain fatty acyl-CoA synthetase (ACSL) activity was assessed by enzyme-linked immunosorbant assay (ELISA). Liver tissues were homogenized in cold PBS with a glass homogenizer on ice. ACSL activity was measured using Rat Fatty Acyl-CoA Synthetase ELISA Kit (Mybiosource, San Diego, CA, USA) in strict accordance with the manufacturer's instructions, and detected using a microplate reader (Bio Tek, Winooski, VT, USA) at 450 nm.

Quantitative Real-Time Polymerase Chain Reaction

Rat liver tissues were homogenized and lysed, and total RNA was isolated with TRIzol reagent (Invitrogen). Reverse transcription was performed with 500 ng of total RNA and Superscript III reverse transcriptase (Invitrogen). Real-time

polymerase chain reaction (PCR) was performed with SYBR Green PCR Master Mix (Applied Biosystems, Foster City, CA, USA). The cDNA subsequently was amplified by PCR using the following thermal conditions: 5 minutes at 95°C, 40 cycles of 95°C for 5 seconds and 60°C for 30 seconds. The sequences of the primers are listed in Table 1. GAPDH or β-actin was used as an internal control for normalization.

Isolation and Quantification of MicroRNA-33

Total RNA was isolated with TRIzol reagent (Invitrogen) and reverse transcribed with Mir-X miRNA First-Strand Synthesis Kit (Clontech, Mountain View, CA). Then, real-time PCR for microRNA (miR)-33 was performed using the following primer: 5′-GTG CAT TGT AGT TGC ATT GCA-3′ (forward). The expression of miR-33 was normalized to expression of U6 snRNA expression.

Western Blot Analysis

Liver tissues were homogenized and lysed on ice with RIPA buffer containing protease inhibitor cocktail (Roche, Branchburg, NJ, USA) and phosphatase inhibitor (Sigma-Aldrich). Protein lysates were seperated by 8% to 15% sodium dodecyl sulfate polyacrylamide gel electrophoresis (SDS-PAGE), transferred to polyvinylidene difluoride membranes (Bio-Rad Laboratories, Hercules, CA, USA), and then blocked in blocking buffer (0.1% Tween20 and 8% bovine serum albumin [BSA] in Tris-buffered saline [TBS]) for 1 hour. Membranes subsequently were

incubated with mouse anti-CPT1A (1:1000, Abcam), rabbit anti-peroxisome proliferator-activated receptor α (PPARα) (1:1000, Abcam), and rabbit anti-GAPDH (1:3000, Santa Cruz Biotechnology, Santa Cruz, CA, USA) at 4°C overnight. After the reaction, membranes were treated with horseradish peroxidase (HRP)-conjugated secondary antibody (anti-rabbit IgG [1:25000, Bio-Rad Laboratories] or anti-mouse IgG [1:25000, Bio-Rad Laboratories]) for 1 hour at room temperature. The bands were detected using enhanced chemiluminescence reagent (Bio-Rad Laboratories).

Adenosine Triphosphate Assay

Adenosine triphosphate (ATP) concentrations of homogenized liver tissue samples were measured using an ATP assay kit (Abcam), according to the manufacturer's instructions and were assessed using a microplate reader (Bio Tek) at 570 nm.

Statistical Analysis

All experiments were conducted in duplicate or triplicate. Data are expressed as mean ± standard deviation. Student's t-tests were performed for group-wise comparisons and $P < 0.05$ was considered statistically significant. Statistical analyses were performed using PASW version 22.0 (SPSS Inc., Chicago, IL, USA).

Table 1. Primer sequences

Gene		Sequence
ACSL 1	forward	5 -AAG CTC TGG AGG ATC TTG GA-3′
	reverse	5′-GGG TTG CCT GTA GTT CCA CT-3′
ACSL 3	forward	5′-TAA AGG CTG ACG TGG ACA AG-3′
	reverse	5′-CCT TTG GAA TTC CTG TGG AT-3′
ACSL 4	forward	5′-ATC TCC CAA AGC TGG AAC AC-3′
	reverse	5′-CTG GTC CCT TAA CGT GTG TG-3′
ACSL 5	forward	5′-TGT AGG GAT TGA GGG AGG AG-3′
	reverse	5′-CAC AGC AAG TCC TCT TTG GA-3′
FATP 1	forward	5′-CCC TGG ATG AGA GAG TCC AT-3′
	reverse	5′-GCA GGA GAA ACA CCT GAA CA-3′
FATP 2	forward	5′-CTC TTT CAG CAC ATC TCG GA-3′
	reverse	5′-CCT CTT CCA TCA GGG TCA CT-3′
FATP 3	forward	5′-CTG GGA CGA GCT AGA GGA AG-3′
	reverse	5′-GCT GAG GCC AGA GGT CTA AC-3′
FATP 4	forward	5′-CGC TGC TGT TCT CCA AGC TGG-3′
	reverse	5′-GAT GAA GAC CCG GAT GAA ACG-3′
FATP 5	forward	5′-GAA GGA ACC TGG AAG CTC TG-3′
	reverse	5′-AGT GTC GAT TTC CGA TTT CC-3′
FATP 6	forward	5′-CAG TAC CAC CAA GCC ATC AC-3′
	reverse	5′-TGG AAC TGG CTA ATC ACA GC-3′
PPARα	forward	5′-AGC CAT TCT GCG ACA TCA-3′
	reverse	5′-CGT CTG ACT CGG TCT TCT TG-3′
CPT1A	forward	5′-GCT TCC CCT TAC TGG TTC C-3′
	reverse	5′-AAC TGG CAG GCA ATG AGA CT-3′
HO-1	forward	5′-TGC ACA TCC GTG CAG AGA AT-3′
	reverse	5′-CTG GGT TCT GCT TGT TTC GC-3′
HO-2	forward	5′-AGG GCA GCA CAA ACA ACT CA-3′
	reverse	5′-TCT GGC TCA TTC TGT CCT AC-3′
β-actin	forward	5′-GGG ACC TGA CTG ACT ACC TCA T-3′
	reverse	5′-ACG TAG CAC AGC TTC TCC TTA AT-3′
Gapdh	forward	5’-TCC CTC AAG ATT GTC AGC AA-3’
	reverse	5’-AGA TCC ACA ACG GAT ACA TT-3’

Results

CP-MSC Transplantation Ameliorates Inflammation in the BDL Rat Liver

To assess the effect of transplantation of CP-MSCs on cholestatic liver injury, BDL rats were divided into 2 groups: rats in the transplanted group were injected with CP-MSCs, and rats in the nontransplanted group were injected with culture medium. As shown in Figure 1, we observed infiltration of inflammatory cells around bile ducts and bile duct proliferation in portal areas in both nontransplanted and transplanted groups 1 week after BDL. Two weeks after BDL, portal areas were expanded as a result of extensive bile duct proliferation, concentric periductal fibrosis, and disorganization of normal lobular structures in the nontransplanted group. Bile duct proliferation was less prominent, and the lobular pattern was preserved in the transplanted group compared to the nontransplanted group (Figure 1). Hepatic steatosis was not observed in control, nontransplanted, or transplanted groups.

CP-MSC Transplantation Attenuates BDL-Induced Hypercholesterolemia but Does Not Affect Fatty Acid Uptake

Obstruction of bile excretion induced by BDL results in overflow of biliary phospholipids in the circulation [4]. Therefore, we explored the effect of transplantation of CP-MSCs on cholesterol metabolism by measuring the cholesterol concentrations in serum. Total cholesterol was markedly elevated in the

nontransplanted group 2 weeks after BDL compared to the control group, whereas it was significantly reduced in the transplanted group compared to the nontransplanted group ($P < 0.05$; Figure 2(a)). Results similar to those for total cholesterol were found for the concentrations of serum LDL cholesterol and triglyceride (Figure 2(a)). Increases in serum levels of total bilirubin, ALP, and CRP were shown to be attenuated after transplantation of CP-MSCs ($P < 0.05$; Figure 3).

Because hypercholesterolemia is induced by chronic cholestasis, we hypothesized that fatty acid uptake into hepatocytes may be altered in BDL rats. ACSLs and fatty acid transport proteins (FATPs) are thought to be essential for the intracellular uptake and transport of fatty acids [15, 16]. Therefore, we determined the activity of ACSLs and the expression levels of ACSLs and FATPs in rat liver tissues. ACSL activity–measured by ELISA–was increased significantly in the transplanted group compared to the nontransplanted group ($P < 0.05$; Figure 2(b)). The expression levels of ACSL1, which is highly expressed in the normal liver [17], were decreased in BDL rats, however, were not increased significantly by CP-MSC transplantation (Figure 2(c)). The expression levels of ACSL4 and ACSL5, which are located in rat liver peroxisomes and mitochondria, respectively [18], declined drastically after BDL and were not restored by CP-MSC transplantation (Figure 4). The expression levels of FATP2 and FATP5, which are expressed in hepatocytes [19, 20], were decreased in BDL rats, and were not increased significantly by CP-MSC transplantation (Figure 2(c) and 5). Collectively, these findings indicate that

cholestasis and hypercholesterolemia induced by BDL are ameliorated by CP-MSC transplantation. However, transplantation of CP-MSCs does not appear to restore processes of fatty acid import into hepatocytes.

CPT1A Expression Is Changed via MiR-33 in BDL Rats

CPT1A is a rate-limiting enzyme located in the mitochondrial outer membrane that catalyzes β-oxidation of free fatty acid [21]. PPARα regulates mitochondrial and peroxisomal fatty acid oxidation by controlling downstream genes, such as CPT1A [22]. We investigated whether the expression of genes associated with fatty acid oxidation are altered in BDL rats and restored by transplantation of CP-MSCs. The mRNA levels of PPARα and CPT1A were remarkably decreased after BDL (Figure 6(a) and (b)). PPARα mRNA levels were similar in nontransplanted and transplanted groups (Figure 6(a)); however, CPT1A mRNA was significantly augmented 2 weeks after CP-MSC transplantation ($P < 0.05$; Figure 6(b)). On the contrary, the increased protein expression levels of CPT1A by BDL were reinstated to near-control levels 3 and 5 weeks after transplantation of CP-MSCs ($P < 0.05$; Figure 6(c)). These results were confirmed by immunofluorescence staining (Figure 6(d)). MiR-33 represses its target genes, which are involved in free fatty acid oxidation, such as CPT1A [23]. To evaluate whether miR-33 is a posttranscriptional regulator of CPT1A in BDL rat liver, we analyzed expression levels of miR-33. As expected, we determined that miR-33 expression was reduced in BDL rats and was restored by transplantation of CP-MSCs (Figure 6(e)). Taken

together, these results suggest that CPT1A may be regulated posttranscriptionally by miR-33 in a PPARα-independent manner.

CP-MSC Transplantation Restores Cellular ATP Production by Regulating Heme Oxygenases

To demonstrate alterations in cellular energy production after BDL, we measured ATP levels in BDL rat liver. ATP production was decreased after BDL but was augmented 1 week after CP-MSC transplantation (Figure 7(a)). Heme oxygenases (HOs) are suggested to be involved in regulating mitochondrial function [24]. Therefore, we assessed the expression levels of HOs in liver tissues. We determined that HO-1 expression was increased substantially in a time-dependent manner post-BDL until week 3. However, the augmented expression of HO-1 reverted to near-control levels 2 weeks after transplantation of CP-MSCs ($P < 0.05$; Figure 7(b)). The HO-2 expression pattern was inversely related to that of HO-1 (Figure 7(c)). These findings implicate that CP-MSC transplantation may ameliorate cellular ATP production via alternative expressions of HO-1 and HO-2.

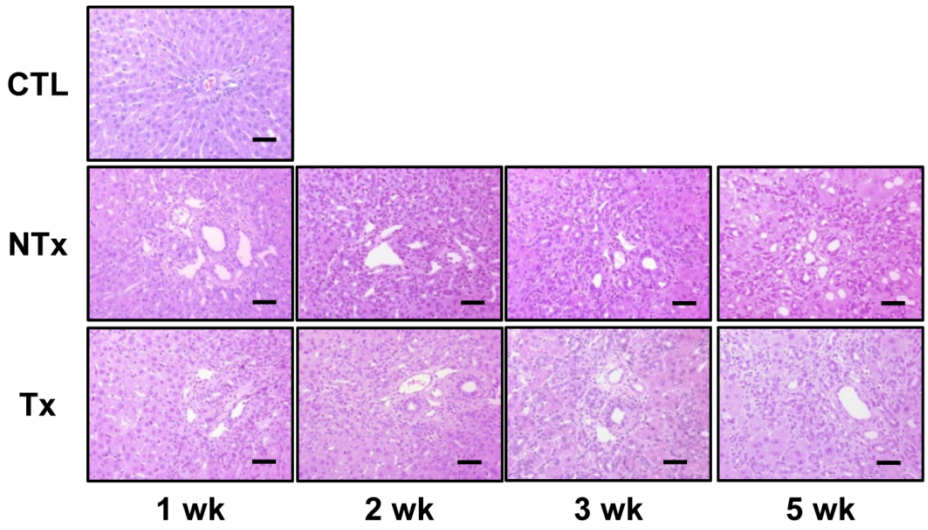

Figure 1. Inflammatory response induced by chronic cholestasis and effect of CP-MSC transplantation. Histologic analysis with hematoxylin and eosin staining (scale bar = 50 μm; original magnification, ×200). CTL, control group; NTx, nontransplanted group; Tx, transplanted group.

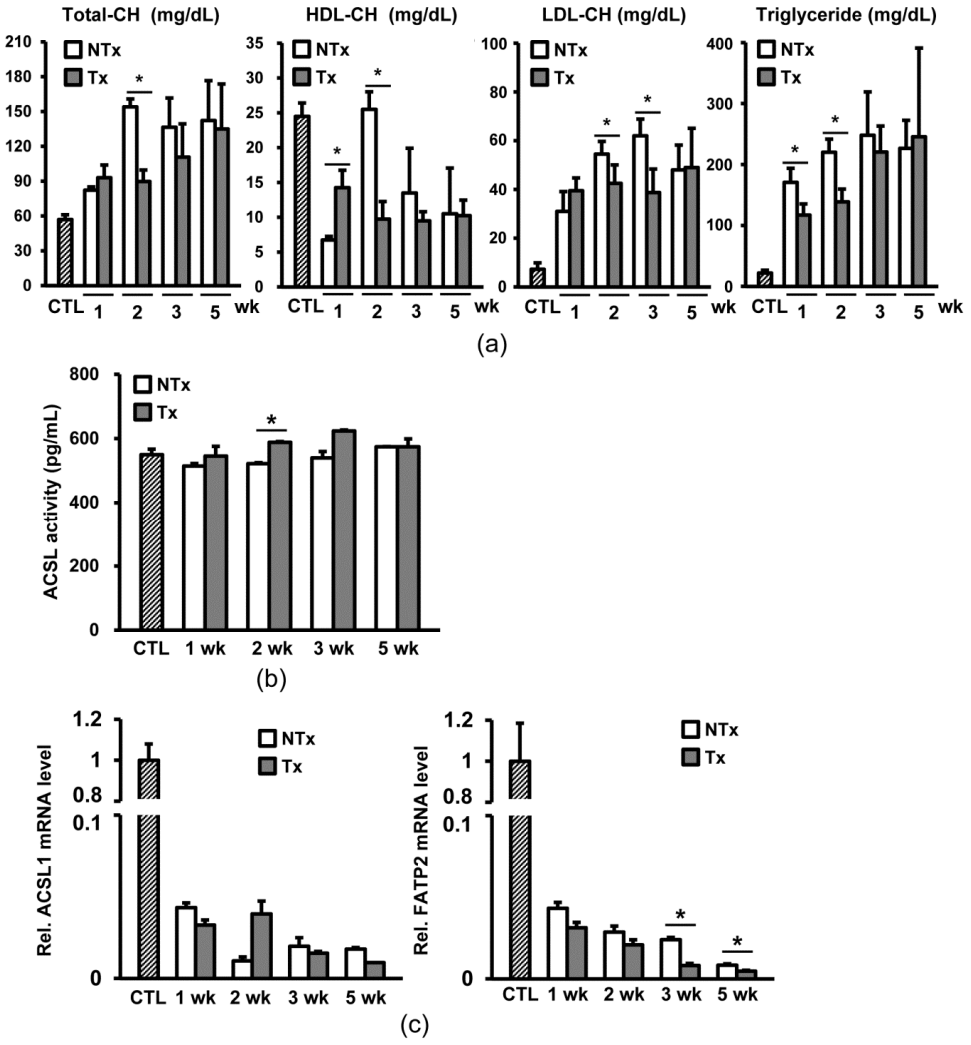

Figure 2. Changes in serum lipid profiles and expression levels of genes associated with intracellular uptake of fatty acids after BDL and/or CP-MSC transplantation. (a) Serum levels of total cholesterol, HDL cholesterol, LDL cholesterol, and triglyceride. (b) Activities of ACSL, as measured by ELISA. (c) mRNA expression levels of ACSL1 (left) and FATP2 (right). β-actin was used as an internal control for normalization. Data are expressed as a fold change related to

the control group. *P < 0.05 (compared to the nontransplanted group). CTL, control group; NTx, nontransplanted group; Tx, transplanted group.

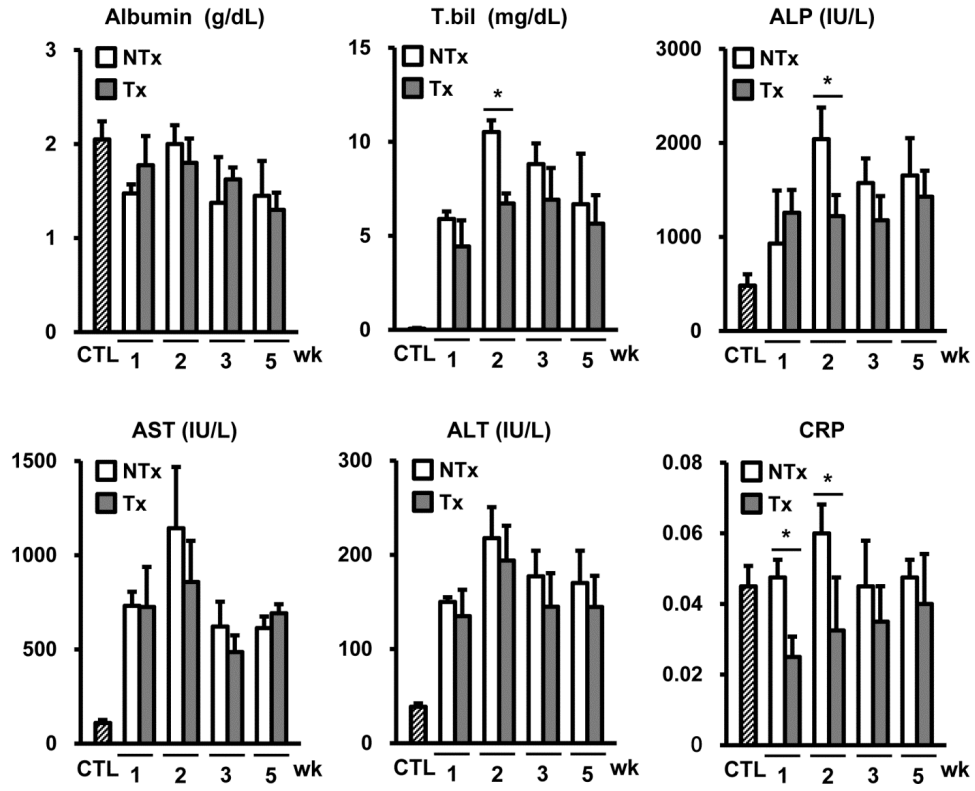

Figure 3. The results of blood chemistry. *P < 0.05 (compared to nontransplanted group). CTL, control group; NTx, nontransplanted group; Tx, transplanted group.

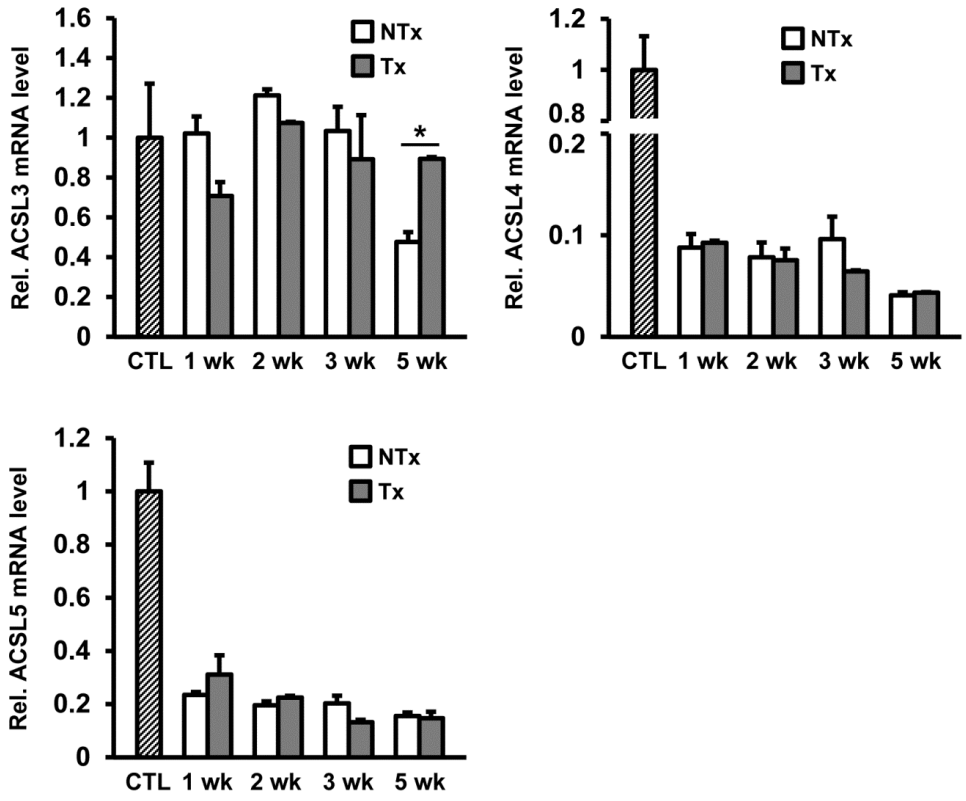

Figure 4. mRNA expression levels of ACSLs. β-actin was used as internal control for normalization. Data are expressed as a fold change related to the control group. **P* < 0.05 (compared to nontransplanted group). CTL, control group; NTx, nontransplanted group; Tx, transplanted group.

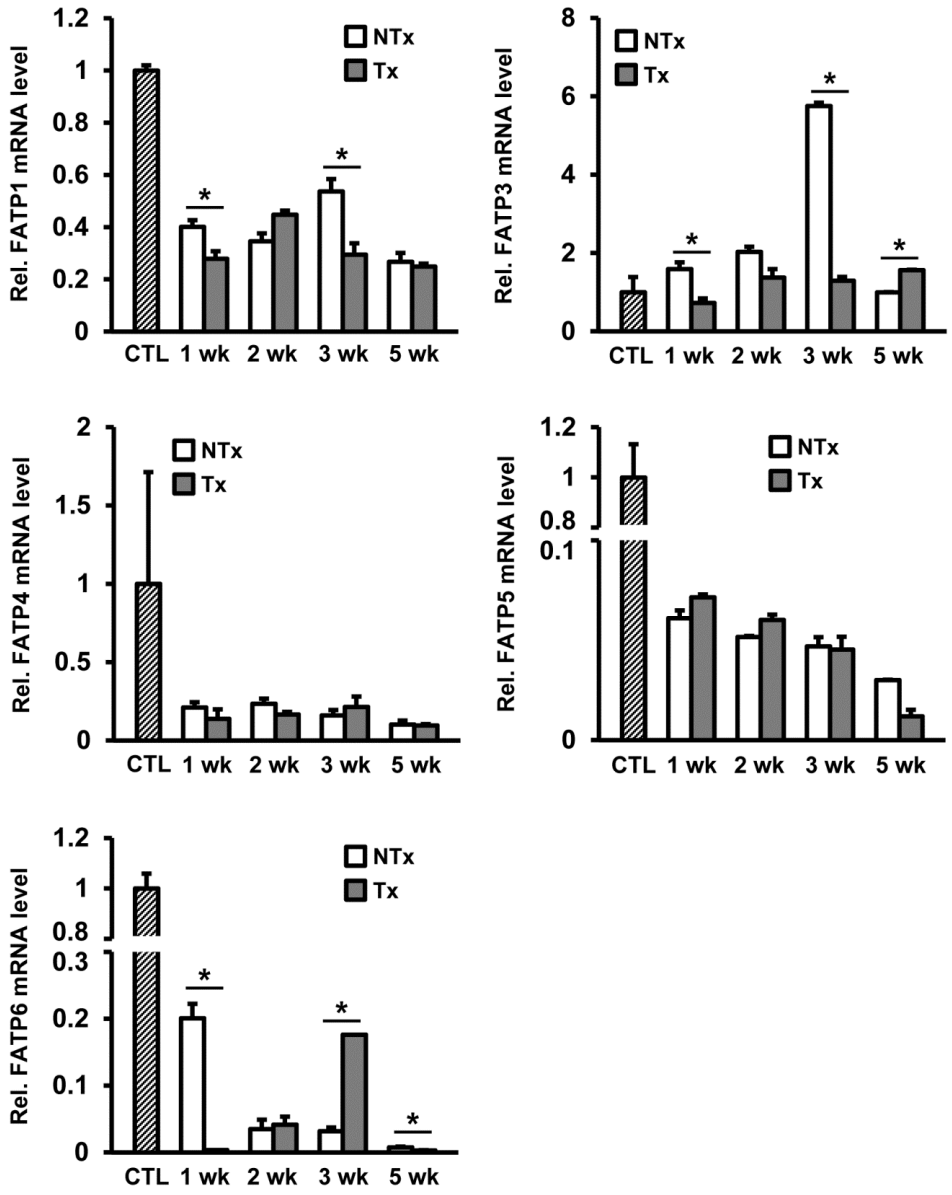

Figure 5. mRNA expression levels of FATPs. β-actin was used as internal control for normalization. Data are expressed as a fold change related to the control group. *P < 0.05 (compared to nontransplanted group). CTL, control group; NTx, nontransplanted group; Tx, transplanted group.

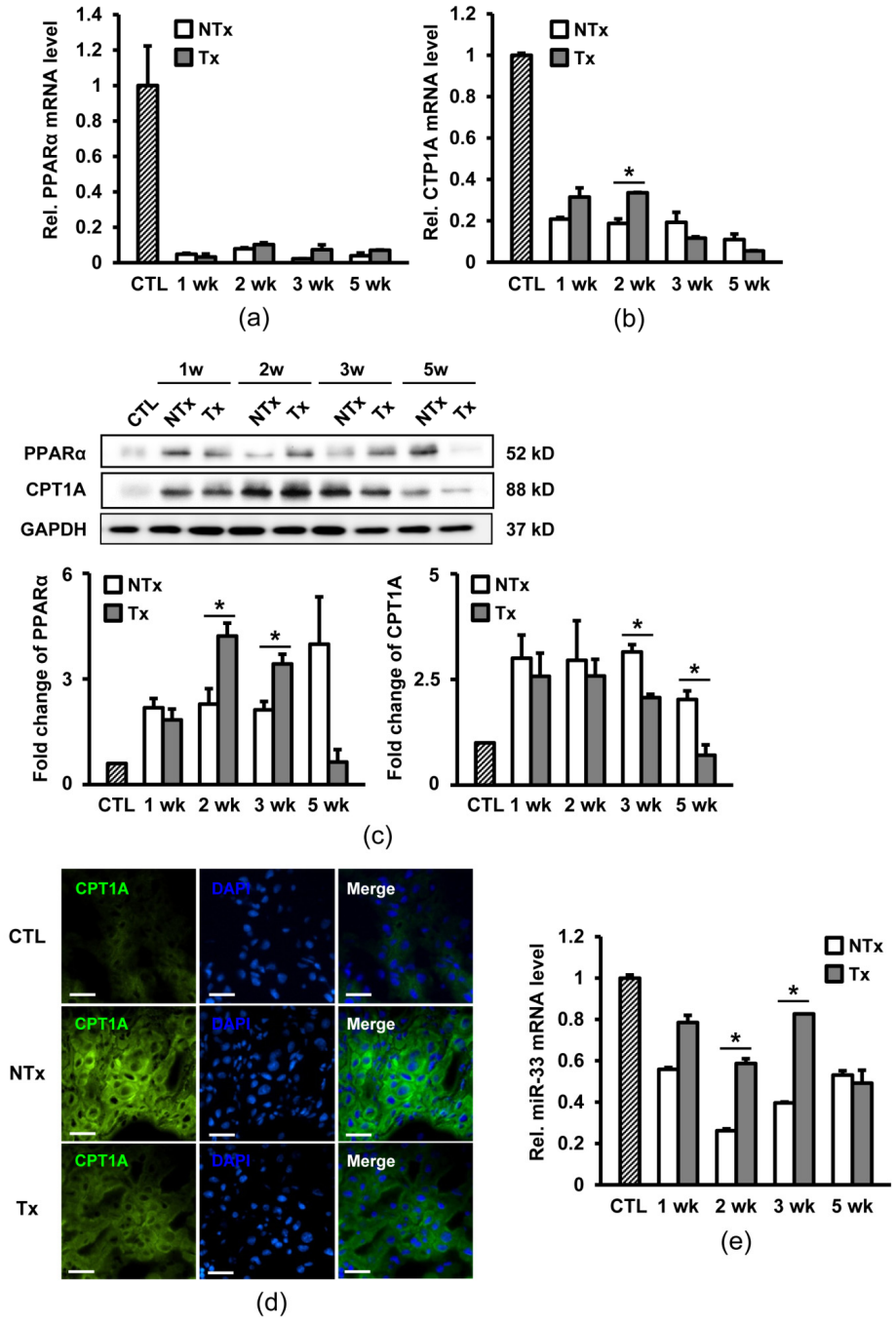

Figure 6. Expression of genes associated with fatty acid oxidation after BDL and/or CP-MSC transplantation. mRNA expression levels of PPARα (a) and

CPT1A (b) by real-time PCR. β-actin was used as an internal control for normalization. Data are expressed as a fold change related to the control group. (c) Protein expression levels of PPARα and CPT1A. GAPDH was used as a loading control and quantification by densitometry of Western blots was normalized to GAPDH. Data are expressed as a fold change related to the control group. (d) Analysis of CPT1A expression with immunofluorescence staining (scale bar = 200 μm; original magnification, ×400). Liver tissues, which were collected at 3 weeks post-transplantation in the transplanted group and post-BDL in the nontransplanted group, were used in immunofluorescence staining. (e) mRNA expression levels of miR-33. U6 snRNA was used as an internal control for normalization. *$P < 0.05$ (compared to the nontransplanted group). CTL, control group; NTx, nontransplanted group; Tx, transplanted group.

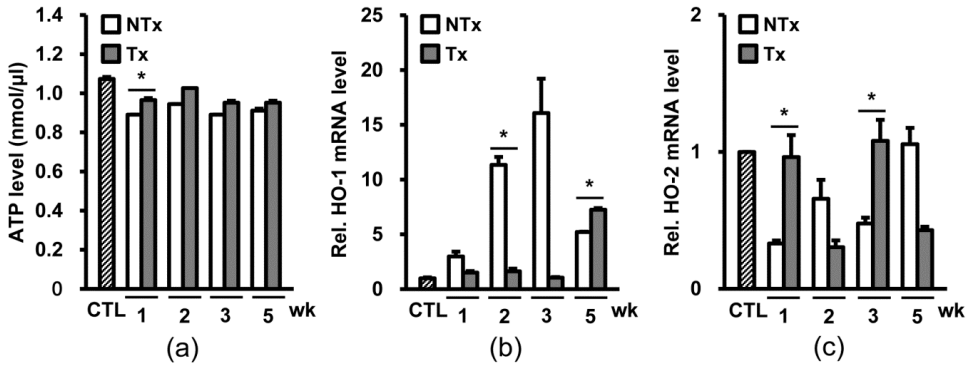

Figure 7. Changes in cellular ATP production and expression levels of HOs after BDL and/or CP-MSC transplantation. (a) Analysis of ATP levels in the liver tissues by ATP assay. mRNA expression levels of HO-1 (b) and HO-2 (c), assessed by real-time PCR. GAPDH was used as an internal control for normalization. Data are expressed as a fold change related to the control group. **P* < 0.05 (compared to the nontransplanted group). CTL, control group; NTx, nontransplanted group; Tx, transplanted group.

Discussion

In this study, we demonstrated that alterations in lipid metabolism in BDL rats might be ameliorated by transplantation of CP-MSCs. Chronic cholestasis, resulting from BDL, led to massive inflammation, hypercholesterolemia, and a drastic decrease in intracellular fatty acid transport; and these changes were partially reverted by CP-MSC transplantation. Regarding mitochondrial β-oxidation, the expression of CPT1A was changed following BDL and CP-MSC transplantation via miR-33, which is known as a posttranscriptional regulator of CPT1A, independent of PPARα. Decreased cellular ATP production after BDL, which reflects mitochondrial dysfunction, was increased by CP-MSC transplantation via regulation of HO-1 and HO-2.

Stem cell therapy with MSCs has been tried for the treatment of various liver diseases, including cirrhosis and hepatic failure, as an alternative to liver transplantation. We previously reported that CP-MSCs had anti-inflammatory, anti-fibrotic, and proregenerative effects in a chronic liver injury model induced by carbon tetrachloride (CCl4) [10, 11]. Liver fibrosis and increased expression of type I collagen and α-smooth muscle actin in CCl4-treated rats were reduced after CP-MSC transplantation, which suggested that CP-MSCs have anti-fibrotic effects [10]. Transplantation of CP-MSCs also showed anti-inflammatory effects of attenuating leukocyte infiltration and augmenting anti-inflammatory cytokine interleukin-10 in liver tissues. In addition, CP-MSC transplantation promoted liver

regeneration through activating autophagy [11]. In our present study, improvement of survival and anti-fibrotic effect was reconfirmed in a BDL rat model (data not shown). Furthermore, we demonstrated a novel effect of CP-MSCs as modulators of hepatic lipid metabolism in BDL rats. Alterations in serum cholesterol profiles and hepatic fatty acid oxidation, which resulted from BDL, were ameliorated after CP-MSC transplantation. Engraftment of transplanted CP-MSCs in the BDL rat liver was verified (data not shown). However, the stem cell fate after engraftment and the mechanisms underlying the therapeutic effect of CP-MSC transplantation on lipid metabolism are still unclear.

Because bile acids play a key role in lipid and energy homeostasis, alterations in lipid metabolism are inevitable in cholestatic liver diseases [4, 5, 25]. De Vriese and colleagues reported the results of lipid analysis of BDL rats and identified hypercholesterolemia and changes in the serum phospholipid profile, in proportion to serum levels of total bilirubin and ALP; however, a decrease in liver fat content in BDL rats was also observed [4]. In a more recent study, a high-cholesterol diet was not found to cause hepatic steatosis in BDL mice [25]. Our study findings of hypercholesterolemia without hepatic steatosis in BDL rats are consistent with these previous studies. Also, we demonstrated that intracellular fatty acid transport was markedly suppressed after BDL. An absence of hepatic steatosis, despite hypercholesterolemia, might be explained by intestinal lipid malabsorption via bile acids combined with suppression of fatty acid import into hepatocytes.

Because the previous studies, which reported the changes in lipid metabolism in

cholestatic liver diseases, focused on lipid malabsorption and cholesterol profiles, alterations in fatty acid oxidation have not been elucidated so far. Mitochondrial β-oxidation is a catabolic process that yields acetyl-CoA from long-chain acyl-CoA; acetyl-CoA then serves as a substrate in ATP generation [26]. Fatty acids, in the form of acyl-CoA, enter mitochondria by CPT1A, a rate-limiting enzyme that catalyzes mitochondrial β-oxidation [21]. Moreover, PPARα has been identified as an upstream regulator of CPT1A [22]. We demonstrated that protein expression of CPT1A was upregulated in BDL rats and was downregulated after CP-MSC transplantation, independent of PPARα. In contrast, mRNA expression of CPT1A exhibited an opposite pattern to CPT1A protein expression. Therefore, we explored the possibility of posttranscriptional regulation of CPT1A and verified that CPT1A is changed via alternative expression of miR-33 [23]. Because mitochondrial β-oxidation is a major source of ATP production in the liver [26], we further analyzed ATP production as an estimation of mitochondrial function. We revealed that decreased ATP production in BDL rat liver was restored by transplantation of CP-MSCs. HOs are thought to be mediators by which CP-MSCs correct mitochondrial dysfunction. Although HO-1 has been suggested to play a role in regulating mitochondrial function [24, 27], further studies are warranted to ascertain whether mitochondrial fatty acid oxidation is regulated by HOs. We have failed to demonstrate a consistent therapeutic effect on ATP production over time after CP-MSC transplantation. It may be worthwhile to transplant CP-MSCs repeatedly to overcome these limitations and to augment the therapeutic effect. Because

mitochondrial dysfunction is not a primary pathophysiologic process in cholestatic liver injury, the efficacy of CP-MSC transplantation on lipid metabolism needs to be further assessed in a model of nonalcoholic fatty liver disease. Nuclear respiratory factors and PPARγ coactivator 1α, which are key factors regulating hepatic mitochondrial function [26], are worth of investigation as a mechanism of therapeutic effect of CP-MSCs.

In our present study, we delineated perturbed lipid homeostasis in a model of chronic cholestatic liver injury. We demonstrated the therapeutic effect of CP-MSC transplantation to ameliorate alterations in lipid metabolism involving mitochondrial fatty acid oxidation. These results provide novel insight into the mechanisms of stem cell therapy and support the therapeutic potential of CP-MSC transplantation in chronic cholestatic liver diseases.

References

[1] M. M. Manos, W. A. Leyden, R. C. Murphy, N. A. Terrault and B. P. Bell, "Limitations of conventionally derived chronic liver disease mortality rates: Results of a comprehensive assessment," Hepatology, vol. 47, no. 4, pp. 1150-1157, 2008.

[2] M. Trauner, P. J. Meier and J. L. Boyer, "Molecular pathogenesis of cholestasis," N Engl J Med, vol. 339, no. 17, pp. 1217-1227, 1998.

[3] K. B. Lee, "Histopathology of a benign bile duct lesion in the liver: Morphologic mimicker or precursor of intrahepatic cholangiocarcinoma," Clin Mol Hepatol, vol. 22, no. 3, pp. 400-405, 2016.

[4] S. R. De Vriese, J. L. Savelii, J. P. Poisson et al., "Fat absorption and metabolism in bile duct ligated rats," Ann Nutr Metab, vol. 45, no. 5, pp. 209-216, 2001.

[5] T. Kamisako and H. Ogawa, "Effect of obstructive jaundice on the regulation of hepatic cholesterol metabolism in the rat. Disappearance of abcg5 and abcg8 mRNA after bile duct ligation," Hepatol Res, vol. 25, no. 2, pp. 99-104, 2003.

[6] D. J. Prockop, "Marrow stromal cells as stem cells for nonhematopoietic tissues," Science, vol. 276, no. 5309, pp. 71-74, 1997.

[7] Y. Fukuchi, H. Nakajima, D. Sugiyama, I. Hirose, T. Kitamura and K. Tsuji, "Human placenta-derived cells have mesenchymal stem/progenitor cell potential," Stem Cells, vol. 22, no. 5, pp. 649-658, 2004.

[8] H. J. Lee, K. E. Cha, S. G. Hwang, J. K. Kim and G. J. Kim, "In vitro screening system for hepatotoxicity: comparison of bone-marrow-derived mesenchymal stem cells and Placenta-derived stem cells," J Cell Biochem, vol. 112, no. 1, pp. 49-58, 2011.

[9] M. J. Kim, K. S. Shin, J. H. Jeon et al., "Human chorionic-plate-derived mesenchymal stem cells and Wharton's jelly-derived mesenchymal stem cells: a comparative analysis of their potential as placenta-derived stem cells," Cell Tissue Res, vol. 346, no. 1, pp. 53-64, 2011.

[10] M. J. Lee, J. Jung, K. H. Na et al., "Anti-fibrotic effect of chorionic plate-derived mesenchymal stem cells isolated from human placenta in a rat model of CCl(4)-injured liver: potential application to the treatment of hepatic diseases," J Cell Biochem, vol. 111, no. 6, pp. 1453-1463, 2010.

[11] J. Jung, J. H. Choi, Y. Lee et al., "Human placenta-derived mesenchymal stem cells promote hepatic regeneration in CCl4 -injured rat liver model via increased autophagic mechanism," Stem Cells, vol. 31, no. 8, pp. 1584-1596, 2013.

[12] M. F. Mahmoud, S. E. Swefy, R. A. Hasan and A. Ibrahim, "Role of cannabinoid receptors in hepatic fibrosis and apoptosis associated with bile duct ligation in rats," Eur J Pharmacol, vol. 742, pp. 118-124, 2014.

[13] J. H. Jun, J. H. Choi, S. H. Bae, S. H. Oh and G. J. Kim, "Decreased C-reactive protein induces abnormal vascular structure in a rat model of liver dysfunction induced by bile duct ligation," Clin Mol Hepatol, vol. 22, no. 3, pp. 372-381, 2016.

[14] J. Jung, J. W. Moon, J. H. Choi, Y. W. Lee, S. H. Park and G. J. Kim, "Epigenetic Alterations of IL-6/STAT3 Signaling by Placental Stem Cells Promote Hepatic Regeneration in a Rat Model with CCl4-induced Liver Injury," Int J Stem Cells, vol. 8, no. 1, pp. 79-89, 2015.

[15] J. Storch and B. Corsico, "The emerging functions and mechanisms of mammalian fatty acid-binding proteins," Annu Rev Nutr, vol. 28, pp. 73-95, 2008.

[16] P. A. Watkins, "Fatty acid activation," Prog Lipid Res, vol. 36, no. 1, pp. 55-83, 1997.

[17] D. G. Mashek, L. O. Li and R. A. Coleman, "Long-chain acyl-CoA synthetases and fatty acid channeling," Future Lipidol, vol. 2, no. 4, pp. 465-476, 2007.

[18] T. M. Lewin, J. H. Kim, D. A. Granger, J. E. Vance and R. A. Coleman, "Acyl-CoA synthetase isoforms 1, 4, and 5 are present in different subcellular membranes in rat liver and can be inhibited independently," J Biol Chem, vol. 276, no. 27, pp. 24674-24679, 2001.

[19] A. K. Heinzer, S. Kemp, J. F. Lu, P. A. Watkins and K. D. Smith, "Mouse very long-chain acyl-CoA synthetase in X-linked adrenoleukodystrophy," J Biol Chem, vol. 277, no. 32, pp. 28765-28773, 2002.

[20] H. Doege, R. A. Baillie, A. M. Ortegon et al., "Targeted deletion of FATP5 reveals multiple functions in liver metabolism: alterations in hepatic lipid homeostasis," Gastroenterology, vol. 130, no. 4, pp. 1245-1258, 2006.

[21] G. Svegliati-Baroni, S. Saccomanno, C. Rychlicki et al., "Glucagon-like peptide-1 receptor activation stimulates hepatic lipid oxidation and restores hepatic

signalling alteration induced by a high-fat diet in nonalcoholic steatohepatitis," Liver Int, vol. 31, no. 9, pp. 1285-1297, 2011.

[22] M. Pawlak, P. Lefebvre and B. Staels, "Molecular mechanism of PPARalpha action and its impact on lipid metabolism, inflammation and fibrosis in non-alcoholic fatty liver disease," J Hepatol, vol. 62, no. 3, pp. 720-733, 2015.

[23] K. J. Rayner, C. C. Esau, F. N. Hussain et al., "Inhibition of miR-33a/b in non-human primates raises plasma HDL and lowers VLDL triglycerides," Nature, vol. 478, no. 7369, pp. 404-407, 2011.

[24] A. Jais, E. Einwallner, O. Sharif et al., "Heme oxygenase-1 drives metaflammation and insulin resistance in mouse and man," Cell, vol. 158, no. 1, pp. 25-40, 2014.

[25] T. Moustafa, P. Fickert, C. Magnes et al., "Alterations in lipid metabolism mediate inflammation, fibrosis, and proliferation in a mouse model of chronic cholestatic liver injury," Gastroenterology, vol. 142, no. 1, pp. 140-151.e112, 2012.

[26] F. Nassir and J. A. Ibdah, "Role of mitochondria in nonalcoholic fatty liver disease," Int J Mol Sci, vol. 15, no. 5, pp. 8713-8742, 2014.

[27] W. Yan, D. Li, T. Chen, G. Tian, P. Zhou and X. Ju, "Umbilical Cord MSCs Reverse D-Galactose-induced Hepatic Mitochondrial Dysfunction via Activation of Nrf2/HO-1 Pathway," Biol Pharm Bull, 2017.

요약 (국문 초록)

배경: 담즙 정체성 간질환에서 담즙 분비가 저해되어 간 지질대사의 불균형을 초래한다. 이 연구에서는 담관결찰 쥐 모델을 이용하여 태반유래줄기세포를 이식한 후, 담즙 정체로 인한 미토콘드리아 베타 산화를 포함한 간 지질대사의 변화 양상을 살펴보고자 하였다.

방법과 결과: 이 연구에서는 쥐의 총담관을 결찰하여 담즙 정체를 유발한 모델을 이용하여 실험을 시행하였다. 태반유래줄기세포 이식군에서 꼬리정맥을 통해 태반유래줄기세포를 이식하였다. 담관결찰 후 혈청 콜레스테롤 농도가 증가하였으며, 태반유래줄기세포 이식군에서는 비이식군과 비교하여 통계적으로 유의하게 혈청 콜레스테롤 농도가 감소하였다. Long-chain fatty acyl-CoA synthetase, fatty acid transport protein와 같은 간세포 내 지질 흡수에 관여하는 유전자 발현은 담관결찰에 의해 감소하였으나, 태반유래줄기세포 이식 후 변화가 없었다. 미토콘드리아 베타 산화를 조절하는 중요 효소인 carnitine palmitoyltransferase 1A (CPT1A)는 담관결찰 후 증가하였다가 태반유래줄기세포 이식 후 감소함을 관찰하였다. CPT1A 발현 정도는 peroxisome proliferator-activated receptor α의 발현과는 독립적으로, CPT1A의 전사후 조절인자로 알려져 있는 microRNA-33의 발현 조절을 통해 변화하였다. 미토콘드리아 기능의 표지자 중 하나인 아데노신3인산의 생성은 담관결찰

후 감소하였으나, 태반유래줄기세포 이식에 의해 회복되었다. Heme oxygenase의 발현 또한 담관결찰 및 태반유래줄기세포 이식 후 통계적으로 유의하게 변화하였다.

결론: 담즙 정체성 간손상이 발생하면 간 지질대사의 변화가 초래되며, 태반유래줄기세포를 이식하면 이러한 변화가 개선될 수 있음을 알 수 있었다. 이러한 연구 결과는 담즙 정체성 간질환에서 태반유래줄기세포 치료의 가능성을 시사하며, 태반유래줄기세포 이식이 체내 에너지 대사에 영향을 미치는 매커니즘을 이해하는데 도움이 되는 결과라 할 수 있겠다.

주요어: 담즙정체, 담관결찰, 태반유래줄기세포, 지질대사, 지방산화, CPT1A, microRNA-33

학번: 2015-30001